CH-99-8-3 (RP-899)

Numerical Study of the Effectiveness of Atrium Smoke Exhaust Systems

George V. Hadjisophocleous, Ph.D., P.Eng. **Gary D. Lougheed, Ph.D.** *Member ASHRAE* **Shu Cao**

ABSTRACT

This paper discusses the numerical study of the effectiveness of atrium smoke exhaust systems. This study is part of a project initiated by ASHRAE and the National Research Council of Canada (NRCC), in which both physical and numerical techniques were employed to determine the effectiveness of such systems and to develop guidelines for their design.

This paper presents numerical predictions obtained using a computational fluid dynamics (CFD) model and compares the numerical results with the experimental data obtained from tests performed in this project. Results are also presented for a real-scale atrium and are compared to the results of the scaled-down models. In addition, comparisons are made between the experimental data and results from a two-zone model, as well as results obtained from empirical correlations.

INTRODUCTION

An atrium within a building is a large open space created by an opening, or series of openings, in floor assemblies, thus connecting two or more stories of a building.[1] This design feature has gained considerable popularity, mainly because of its visual appeal. The sides of an atrium may be open to all floors, open to some of the floors, or closed to all or some of the floors by unrated or rated fire-resistant construction. Also, there may be two or more atria within a single building, all interconnected at the ground floor or on a number of floors.

By interconnecting floor spaces, an atrium violates the concept of floor-to-floor compartmentation, which is intended to limit the spread of fire and smoke from the floor of fire origin to other stories inside a building. With a fire on the floor of an atrium or in any space open to it, smoke can fill the atrium and connected floor spaces. Elevators, open stairs, and egress routes that are within the atrium space can also become smoke-laden.

Protecting the occupants of a building from the adverse effects of smoke in the event of a fire is one of the primary objectives of any fire protection system design. Achieving this objective becomes more difficult when dealing with very large spaces, such as an atrium or an indoor sports arena, where a large number of occupants may be present and the compartment geometry may be complex. Because of these difficulties, model building codes place restrictions on the use of atrium spaces in buildings. Some of the requirements, which are commonly applied in codes for buildings with atria, include:

- the installation of automatic sprinklers throughout the building,
- limits on combustible materials on the floor of an atrium,
- the installation of mechanical exhaust systems for use by firefighters, and
- the provision of smoke management systems to maintain tenable conditions in egress routes.

1. For the purposes of this paper, the definition of "atrium" will be in accordance with that used in NFPA 92B (1995) and by Klote and Milke (1992), that is, a large volume space in a commercial building. This includes office buildings, hotels, and hospitals with typical atrium spaces, covered malls, and other buildings with similar large volume spaces. It does not include warehouses, manufacturing facilities, or other similar spaces with high fire load densities.

George V. Hadjisophocleous and **Gary D. Lougheed** are senior research officers and **Shu Cao** is a technical officer in the Fire Risk Management Program, Institute for Research in Construction, National Research Council Canada, Ottawa, Ontario.

Atrium smoke management systems have become common in recent years, and design information for these systems is provided in *NFPA 92B, Guide for Smoke Management Systems in Malls, Atria, and Large Areas* (NFPA 1995) and Klote and Milke (1992). In addition, two of the U.S. model codes (BOCA 1996; ICBO 1994) have recently adopted smoke management system requirements based on *NFPA 92B*.

There are, however, a number of situations that may impact the effectiveness of the smoke management system. These include obstructions in the smoke plume (Hansel and Morgan 1994) or the formation of a pre-stratification layer in the atrium (Klote 1994). In the former case, smoke may be directed to adjacent spaces or mixed with the air within the zone in which tenable conditions are required. In the latter case, the smoke produced by the fire may not reach the ceiling where it could be exhausted by a smoke management system. Also, in this case, smoke buildup could occur at a height at which it can migrate into the communicating spaces.

Under some conditions, another phenomenon may impact the effectiveness of a smoke management system: air from the lower (cold) layer can mix with the smoke in the upper layer as it is being exhausted by the smoke management system. This phenomenon reduces the effectiveness of the smoke management system (Hinckley 1995). As a result, the clear height in the atria is reduced and people in some spaces may be exposed to smoke and toxic fire gases. This phenomenon is referred to as "plugholing" and investigations have been carried out on natural venting systems (Morgan and Gardiner 1990; Spratt and Heselden 1974). To study the effects of plugholing on a mechanical exhaust system used for atrium smoke management, a joint research project was initiated by ASHRAE and the National Research Council of Canada (NRCC) in 1995. This project includes both physical and numerical modeling of an atrium smoke management system. The objective of the project is to develop methods with which designers can account for the mixing of cold air with the smoke exhaust. These methods will provide a basis for the design of cost-effective smoke management systems that will meet design expectations.

This paper presents the results of the atrium project. This includes the results of tests with two atrium physical models. The smaller-scale experiments were conducted in a facility that had a clear height of approximately 5.5 m. All dimensions for the second facility were approximately two times those of the smaller test arrangement. The clear height was approximately 12.5 m. Both atrium physical models included mechanical exhaust systems.

A commercially available computational fluid dynamics (CFD) model was used to model an atrium smoke management system. A comparison between experimental data and the CFD model predictions are provided in this paper. In addition, comparisons are made with results obtained using a two-zone model and empirical correlations.

STEADY-STATE DESIGN FIRES

Klote and Milke (1992) recommend design fires of approximately 2,000 kW and 5,000 kW for atria with restricted fuel and atria with combustibles, respectively. These design fires are similar to those required in the BOCA (1996) and UBC (ICBO 1994) building codes and are used as the basis for the studies discussed in this paper.

DESCRIPTION OF SMALL-SCALE FACILITY

The small-scale experimental facility used for this study was a large compartment with dimensions of 9 m × 6 m × 5.5 m in height. The interior wall surface of the compartment was insulated using 25 mm thick rock fiber insulation. The insulation was used for two reasons: first, to protect the walls of the facility so that high gas temperatures could be attained during the tests and, second, to provide a better boundary condition for the CFD runs.

A fan was used to supply fresh air into the compartment through openings in the floor around the walls. The openings were designed to maintain the velocity of the incoming air to less than 1 m/s for the maximum airflow expected, which was between 2 m^3/s and 4 m^3/s. These openings had a width of 0.1 m and a total length of 22.8 m.

Thirty-two exhaust inlets with a diameter of 150 mm were located in the ceiling of the compartment. These inlets were used to extract the hot gases from the compartment during the tests. All exhaust ducts were connected to a central plenum. A 0.6 m diameter duct was used between the plenum and an exhaust fan. By using multiple exhaust inlets, smoke exhaust system parameters such as total area of exhaust inlet, velocity at the inlets, and exhaust inlet location relative to the ceiling and the fire could be readily investigated.

The exhaust system included a two-speed fan with nominal capacities of 3 m^3/s and 4 m^3/s. The actual volumetric flow rate produced by the fan in a test depended on a number of factors including smoke temperature and the number of exhaust inlets used. Therefore, the volumetric flow rate in the main duct was continuously measured throughout a test.

A square propane sand burner was used for the fire source. The burner was capable of simulating fires ranging from 15 kW to 1,000 kW with three possible fire areas: 0.145 m^2, 0.58 m^2, and 2.32 m^2. The heat release rate of the fire was determined using two methods. The first method computes the heat release rate from the volume flow rate of propane supplied to the burner. The second method was based on the oxygen depletion method using oxygen concentrations, temperature, and volume flow rate measured in the main exhaust duct.

The room was instrumented with thermocouples and pitot tubes for velocity measurements. Also, gas inlets were located in the room for extracting gas samples to determine CO_2 concentrations at various locations.

Twelve CO_2 inlets were located at one of the room quarter points at various heights. The CO_2 inlets were connected to two CO_2 analyzers. A set of 19 thermocouples was located at

the center of the room over the propane burner and eight thermocouples were located along the vertical centreline. Six thermocouples were located at 250 mm intervals along a horizontal line at a height of 3 m and another five thermocouples were located at 250 mm intervals along a horizontal line at a height of 4.5 m. Four additional thermocouples were located along a horizontal line near the ceiling at 1 m intervals.

A second set of thermocouples was located below one of the duct inlets. These thermocouples were used to measure the gas temperatures around the exhaust inlets to determine whether fresh air was exhausted from the room. A thermocouple tree was located at the southwest quarter point with 15 thermocouples. These thermocouples, together with the CO_2 measurements at the same locations, were used to determine the depth of the hot layer in the room.

The volume flow rate, temperature, CO, CO_2, and oxygen concentrations were measured in the main exhaust duct. These measurements were used to determine the heat release rate of the fire, as well as to calculate the exhaust rate of the ventilation system. A pitot tube and thermocouple, located at the center of the duct, were used to determine the volumetric flow rate in the duct. A pitot traverse was conducted prior to the test program. A shape factor for the duct of 0.91 was determined. More details of the small-scale facility and the instrumentation can be found in Lougheed and Hadjisophocleous (1997).

The tests described were conducted over an extended period of time (up to one hour). The test procedure was as follows:

1. All systems, including the mechanical exhaust system and data acquisition system, were started.
2. The small burner was ignited and the propane flow rate adjusted to provide a low heat release rate fire.
3. All conditions in the test facility, except CO_2 concentrations, were monitored continuously using the data acquisition system.
4. The conditions in the test facility were allowed to stabilize for approximately 15 minutes, producing a steady clear height with upper layer exhaust.
5. The CO_2 concentrations at various heights were measured. These data, along with the temperatures measured at the same heights, were used to determine the height of the smoke layer.
6. The heat release rate was increased and Steps 3 through 5 were repeated.

Using this test procedure, data could be acquired for several heat release rates under the same test conditions.

DESCRIPTION OF LARGE-SCALE FACILITY

The large-scale test facility had dimensions approximately two times those of the small-scale test facility described above and was used for a second series of physical model experiments.

The large-scale facility was approximately 12 m × 18 m. It was constructed in one corner of the large-scale hall that has a clear height of 12.5 m. Two sides of the facility were the exterior walls of the hall. The other two sides were formed using draft curtains constructed using solid glass fiber insulation mounted in a lightweight steel frame. The steel frame was attached to cables connected to the ceiling and floor of the hall and were spaced at 4 m intervals. The lower 3 m of the interior partitions were left open to the main hall facility to provide ventilation to the test area.

A 1.2 m diameter duct was attached below the ceiling of the atrium test facility. This duct entered the test facility through the north interior partition. For the test arrangement modeled, a 90° elbow was connected to the south end of this duct. Extensions were connected to this elbow to provide a single exhaust inlet at various heights above the floor.

The north end of the central duct was connected to a vertical duct using two 45° elbows. Two additional 45° elbows were used to connect the lower end of the vertical duct to a horizontal duct at floor level. This duct connected the exhaust system to a fan located at the exterior of the building. A measuring station including a thermocouple, pitot tube, and gas sampling inlet at the center of the duct was located midway between the last elbow in the duct system and the fan to measure volumetric flow rate and heat release rate.

A square propane sand burner was used for the fire source. The burner was capable of simulating fires ranging from 250 kW to 5,000 kW with four possible fire areas: 0.145 m^2, 0.58 m^2, 2.32 m^2, and 9.3 m^2. The heat release rate of the fire was determined using two methods. The first method computes the heat release rate from the volume flow rate of propane supplied to the burner. The second method was based on the oxygen depletion method using oxygen concentrations, temperature, and volume flow rate measured in the main exhaust duct.

With the small heat releases and large volumetric flow rates used for a number of tests, the depletion of oxygen in the exhaust gases was at or below the level for accurate heat release rate measurements using the oxygen depletion method. For these cases, the heat release rate was determined using the measured flow rate of propane into the burner. The oxygen depletion method was used to verify the heat release rate results for the larger fires.

The room was instrumented with thermocouples and pitot tubes for velocity measurements. More details of the room and its instrumentation can be found in Lougheed et al. (1999).

The volume flow rate, temperature, CO, CO_2, and oxygen concentrations were measured in the main exhaust duct. These measurements were used to determine the heat release rate of the fire, as well as to calculate the exhaust rate of the ventilation system. A pitot tube and thermocouple located at the center of the duct system were used to determine the volumetric flow rate in the duct.

NUMERICAL MODELING

This section describes the model used for the numerical simulations, as well as some of the approaches used in modeling both the small-scale and large-scale test facilities and the fire and calculating the interface layer.

Description of the CFD Model

The numerical simulations for this project were done using a general three-dimensional computational fluid dynamics (CFD) model with capabilities in handling laminar and turbulent flows, incompressible and compressible, multicomponent fluids, porous media, Lagrangian particle tracking, reacting combusting flows, conjugate heat transfer, surface-to-surface radiation, and rotating frames of reference and subsonic and transonic and supersonic flows (ASC 1994). The grid generation features of this commercial CFD model include the ability to handle non-orthogonal boundary-fitted grids, grid embedding, and grid attaching.

Turbulence was modeled using the k-ε turbulence model, which is the model used for most engineering applications and found in most commercial codes.

Radiation exchange between the hot gases and the surroundings was modeled using the diffusion radiation model of the commercial CFD model (ASC 1994) with a gas absorption coefficient of 0.1.

Fire Modeling

The fire was modeled using two methods: a flamelet combustion model (Peters 1984, 1986) and a heat source. In the flamelet model, only two user-defined scalar equations are used: one is the mixture fraction and the other is the variance of the mixture fraction. In this simulation, propane was used as fuel and the following 12 chemical species were used from the commercial CFD model's libraries: C_3H_8, O_2, H, O, H_2, H_2O, CO, CO_2, CH_3, CH_4, C_2H_2, and C_2H_4. When using the heat source method, the fire heat release rate was defined as a volumetric heat source in control volumes at the fire location.

Computational Grid

Experimental tests were performed in two facilities. A small-scale facility and a large-scale facility with dimensions approximately double those of the small-scale dimensions. Both of these facilities were modeled using CFD.

Small-scale physical model. Results from the experiments and preliminary numerical simulations indicated that the conditions in the room were symmetric, so the room was modeled by considering only one-quarter of the room. Two different computational grids have been employed. When the flamelet model was used, the computational domain was divided into a grid of 21 × 31 × 21 control volumes. Additional grid points were embedded around the fire and the exhaust outlets to enable better resolution of the solution in these areas. The total number of grid points for these simulations was 24,014. When the volumetric heat source was used for the fire, the computational domain was divided into a grid of 23 × 17 × 24 control volumes. The total number of grid points for these simulations was 9384.

Large-scale physical model. The computational domain used for the large-scale simulations was the entire test room. The computational domain was divided into a grid of 31 × 23 × 23. An embedded grid was used in the region surrounding the exhaust vent to obtain a better resolution in this area. The total number of grid points for these simulations was 30,149.

Boundary Conditions and Fluid Properties

To model the experimental facilities, the following boundary conditions were used:

1. *Solid walls.* The walls of the enclosure were modeled as solid, adiabatic, and hydrodynamically smooth boundaries. This type of boundary is appropriate as the walls of the enclosure were insulated and had a smooth surface.
2. *Symmetry planes.* For small-scale modeling, experiments and preliminary runs indicated that the flow in the room is symmetric, hence, only a quarter of the room was considered for the simulations with symmetric boundary conditions used at the symmetry boundaries. This boundary type was not applied for large-scale modeling because the whole room was modeled.
3. *Ceiling vents.* At the ceiling vents, a constant mass flow rate was assigned based on the experimental data obtained at the quasi-steady state.
4. *Floor openings.* At the floor openings, the total pressure was set to 101325 Pa across the area of the openings. The inlet velocities are free to develop corresponding to the mass flow rate downstream. Inlet air temperature was assumed to be 291 K. Although in the experiments a fan was used to supply fresh air to the room through these openings, the supply air had a very low velocity, and the governing parameter was the flow rate of the exhaust fan, so the assumed boundary condition is acceptable.
5. *Wall openings.* At the open part of the walls surrounding the large-scale facility, a pressure boundary was used that allowed flow in and out of the domain.

Heat Release Rates

The heat release rates used in the numerical simulations were extracted from the experimental data. During the experiments, the propane flow rate was adjusted to a predetermined level to produce the required heat release rate. Figure 1 shows results of a test with a total heat release rate of approximately 25 kW in the initial stage and 225 kW in the final stage of the test. The fire was maintained steady for about 15 minutes at each heat release rate to allow stable conditions to be reached in the test facility. Temperature measurements in the room were used to determine whether stable conditions were reached. For the lower heat release rates, the temperatures in the hot layer quickly stabilized to a relatively steady condition. For the higher heat release rates (>200 kW), however, due to

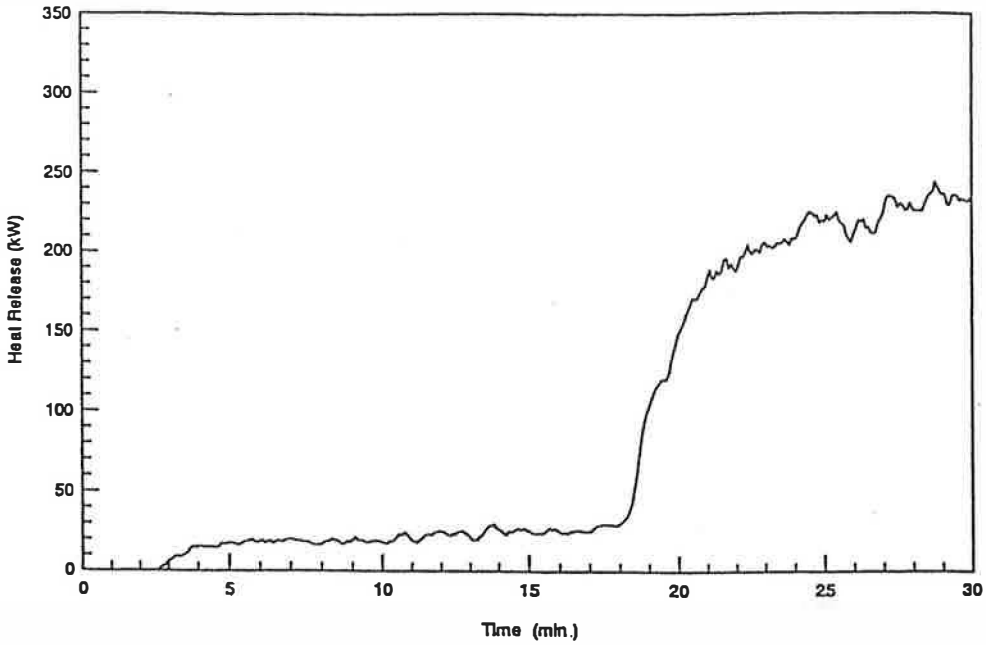

Figure 1 *Experimental heat release rate.*

radiation from the fire, the temperature profiles in the upper layer did not reach a steady condition. However, after 10 minutes with a steady heat release rate, the temperature increase was minimal and it was assumed to be approximately steady.

The steady period determined from the temperature measurements was used to estimate a mean heat release rate, which was the rate used in the numerical simulations.

Hot Layer Interface

The interface height in a compartment such as an atrium is one of the important parameters used in both fire-safety design guides and building codes. This parameter is usually used as a life-safety criterion for evaluating fire protection designs. In designing a smoke management system in an atrium, it is usually required that the smoke management system maintain an interface height of 1.8 m to 3 m above the floor during the time needed for evacuation. Using zone models or simple correlation, interface heights are computed directly; however determining interface heights and smoke layer thickness from experimental data or from results of field models is quite challenging. In both cases, the results may not show a clear transition from the cold layer to the hot layer, so determining the interface is not easy. This is an area where further work has to be done to define a procedure that will be acceptable by fire safety practitioners.

In this study, the procedure described in Cooper et al. (1982) and Peacock and Baubraukas (1991) is used. They have developed a method for defining the height of the interface between the hot and cold zones produced by a fire based on a limited number of point temperature measurements over the height of a compartment. For these calculations, it is assumed that the interface is at the height where the temperature, T_n, is given by:

$$T_n = C_n(T_{max}-T_b) + T_b \qquad (1)$$

where

T_{max} = the maximum temperature or CO_2 concentration,

T_b = the temperature or CO_2 concentration near the bottom of the compartment,

C_n = interpolation constant typically in the range of 0.15 to 0.2.

In this study, a clear height is defined using Equation 1 with C_n set at 0.2. In addition, an interface height is defined with C_n set equal to 0.5. Both temperatures and CO_2 concentrations were used in Equation 1, so two interface heights are defined, one based on temperature and the other on CO_2. As there is variation of the temperature and CO_2 profiles at different locations, the clear and interface heights were computed at each location, and their average value was used to represent the room clear and interface heights.

RESULTS

This section discusses the results obtained from the CFD model for both the small-scale and the large-scale facilities. In addition, comparisons are made with experimental data obtained from the test conducted in these facilities, as well as with predicted results from a real-scale facility representing a real-size atrium. Simulations were also performed to help identify numerical paramcters that may affect the CFD results.

Simulations of Small-Scale Facility

Numerical simulations of the small-scale facility were performed using both the flamelet combustion model and a heat source to define the fire.

For the simulations employing the combustion model, propane was used as the fuel. Propane was introduced at the fire location at a rate corresponding to the heat release rate (HRR) of the fire being considered. The area over which propane was introduced was similar to the area of the pan used in the tests. As only a quarter of the room was used for the small-scale simulations, the HRR simulated was one-fourth of the HRR of the tests. The simulations followed a transient approach and continued until steady-state conditions were established in the room. Typically, it took five minutes of simulation time to obtain a steady solution.

Tables 1 and 2 list the simulations conducted for the small-scale facility. Altogether, 15 tests were done using the flamelet model of the commercial CFD model (ASC 1994) and propane as the fuel. The parameters considered for these simulations were the location of the vent and the HRR of the fire. Three vent locations were modeled, one with the vent near the ceiling, the second with the vent 1 m below the ceiling, and the third with the vent 2 m below ceiling. The heat release rates used were taken from the experimental data by averaging over the steady-state period of the test. The table also lists the calculated clear layer and interface heights and the average temperature of the hot and clear layer.

Figure 2 shows velocity vectors on a vertical plane passing through the ceiling exhaust for Case 2. The results shown are at a steady-state condition, which was achieved five minutes into the simulation. The figure clearly shows the fresh incoming air through the floor inlets flowing upward toward the mid-height of the room before it loses its momentum and turns downward. Figure 2 also shows the strong flow at the ceiling exhaust.

Figure 3 shows temperature contours on the same vertical plane passing through the ceiling exhaust. The figure clearly indicates the hot layer with high temperatures and the lower cold layer, which is at ambient temperature. The figure also shows that the exhaust vent does not significantly affect the temperature contours, indicating that it only draws in gases from the upper region of the hot layer.

The velocity vectors on a vertical plane passing through the fire are shown in Figure 4. The figure shows the fire plume as well as the entrainment of air into the plume. In addition, near the ceiling, a clearly defined ceiling jet is formed that creates a recirculating zone within the hot layer. Figure 5 shows the temperature contours on the same plane and the high temperatures in the fire plume.

Figure 6 shows predicted and experimental temperature profiles along the quarter point of the room, as well as the location of the hot layer and the mean temperatures of the hot and

TABLE 1
Numerical Simulations of Small-Scale Facility Using Flamelet Combustion Model

Exhaust Location	Case	Heat Release Rate (kW)	Mass Flow Rate (kg/s)	Clear Layer Height (m)	Transition Layer Thickness (m)	Clear Layer Temp. (°C)	Hot Layer Temp. (°C)
Vent at Ceiling	1	22	1.19e-4	3.85	4.40	19.93	27.50
	2	48	2.59e-4	3.58	3.85	21.56	38.06
	3	135	7.28e-4	2.20	2.75	25.78	76.77
	4	225	1.21e-3	1.65	2.2	31.22	120.43
	5	280	1.51e-3	1.37	1.92	34.21	145.09
Vent 1.0 m Below Ceiling	6	55	2.97e-4	3.30	3.58	17.05	37.36
	7	155	8.36e-4	1.37	1.65	19.53	68.86
	8	300	1.62e-3	0.82	1.10	23.50	136.23
	9	25	1.35e-4	2.75	3.02	15.14	22.11
	10	225	1.21e-3	1.65	2.47	24.47	110.07
Vent 2.0 m Below Ceiling	11	30	1.62e-4	2.19	2.46	17.85	30.02
	12	63	3.40e-4	1.92	2.19	19.27	44.43
	13	148	7.98e-4	1.10	1.37	21.77	77.57
	14	237	1.28e-3	0.82	1.37	25.44	116.11
	15	285	1.54e-3	0.82	1.37	26.68	139.50

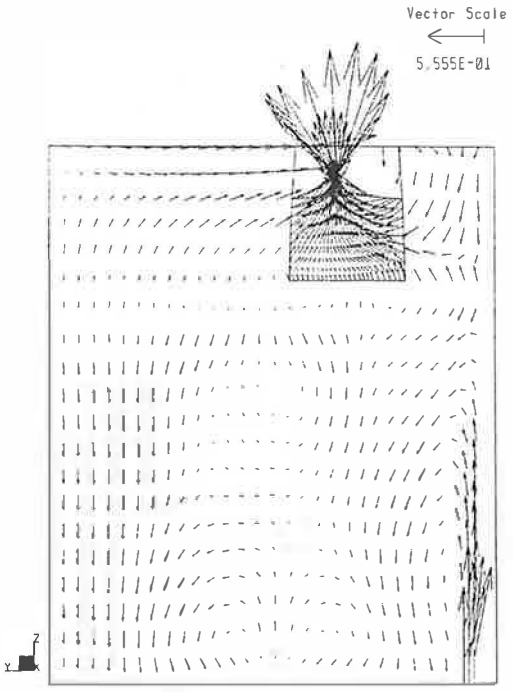

Figure 2 *Velocity vectors for medium scale through ceiling vent (m/s).*

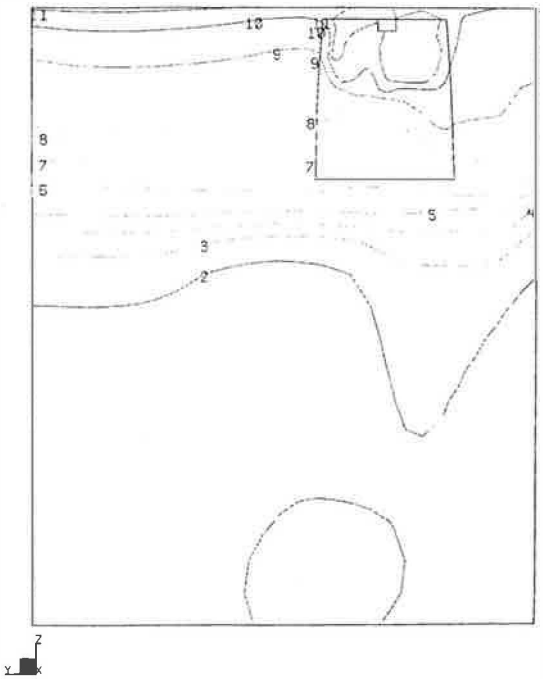

Figure 3 *Temperature contours for medium scale through ceiling vent; contour 2 at 21.60°C and temperature difference between contours 2.78°C.*

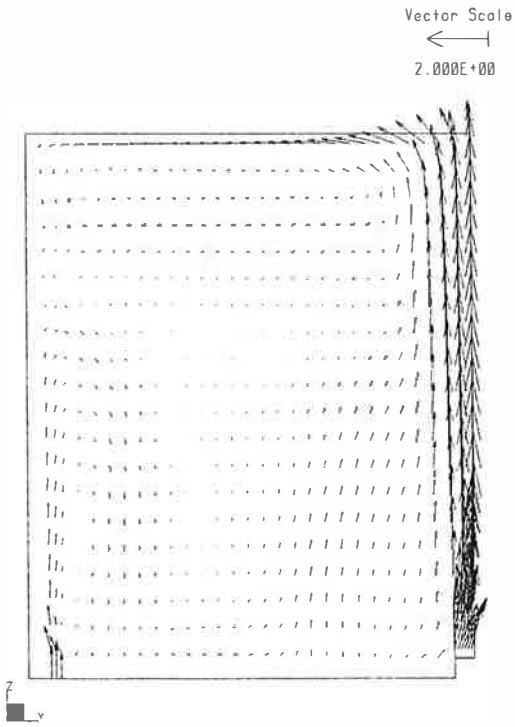

Figure 4 *Velocity vectors for medium scale through fire plume (m/s).*

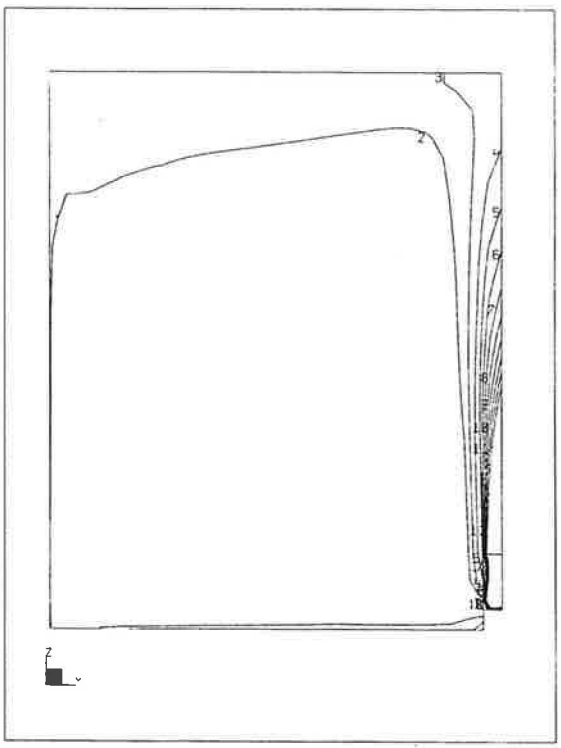

Figure 5 *Temperature contours for medium scale through fire plume; contour 2 at 39.09°C and temperature difference between contours 21.09°C.*

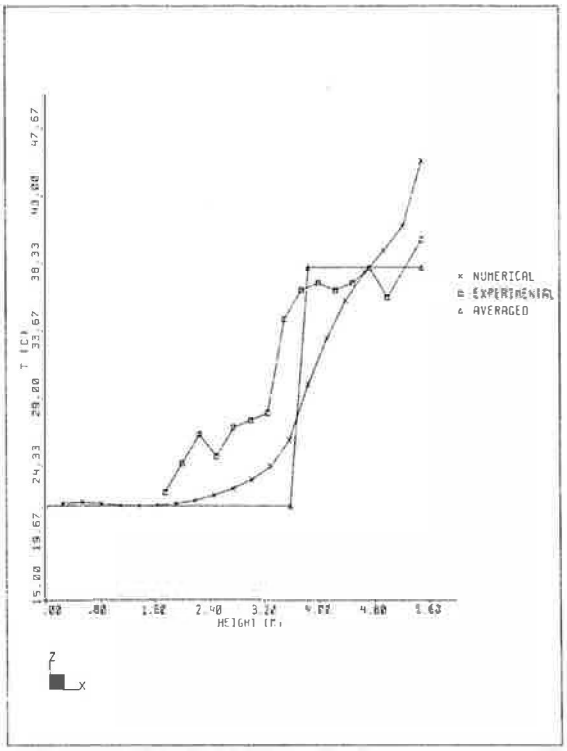

Figure 6 *Comparison between experimental data and model predictions.*

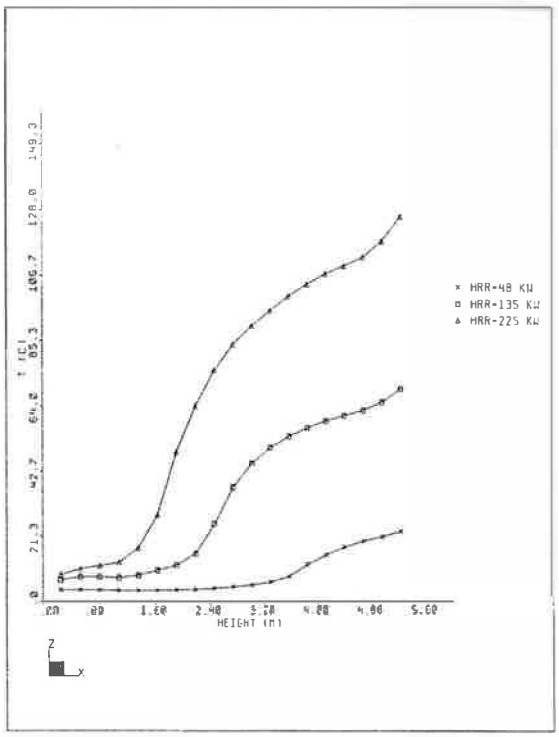

Figure 7 *Effect of HRR on temperature profiles.*

cold layers. Although the predictions appear to be realistic, a significant difference exists between the numerical and the experimental profiles, especially in the hot layer. In this region, the experimental temperature is quite uniform and the interface between the hot and cold layers is clearly defined. The predicted temperature profile shows that the temperature increases with height and does not have a layer with uniform temperature. The average computed temperature in the hot layer, however, compares well with the experimental temperature.

Considerable effort was devoted to find out why the predicted temperatures in the hot layer are not as uniform as the experimental data. Many simulations were performed in which the input parameters were reexamined and a number of different boundary conditions were considered. In addition, simulations were performed with various grid sizes and grid configurations, as well as with and without the radiation model. These efforts, however, did not lead to any significant improvement of the solution.

Parametric Study

A series of runs was performed to determine the impact on the solution of two parameters used in defining the fire as a heat source: the fire area and the fire height. These two parameters define the volume of the fire, which is the volume within which heat is added to the domain as a heat source.

Figure 7 compares temperature profiles at the room quarter point for three different heat release rates: 48 kW, 135 kW, and 225 kW. For all runs, the exhaust vent was located near the ceiling. Figure 8 shows the average temperature in the clear and hot layers and Figure 9 depicts the clear and interface heights for the three cases. As expected, the higher the heat release rate, the higher the temperatures of the hot layer. Also, with the higher heat release rates, the smoke interface is lower in the compartment.

Figure 10 is a plot of the temperature profiles for three simulations with different exhaust vent locations: at the ceiling, 1 m below the ceiling, and 2 m below the ceiling. The heat release rate for these runs was 55 kW. The profiles illustrate that with the exhaust inlet below the ceiling, the hot layer thickness and the temperature in the hot layer increase. Figures 11 and 12 illustrate more clearly the effect of the exhaust vent location on the clear and interface height and average temperature.

Simulations for the Large-Scale Physical Model

A simulation of the large-scale physical model was performed using a volumetric heat source to model the fire. The exhaust inlet was located 2 m below the ceiling. The heat release rate of the heat source employed in the simulation was 4 MW, and the exhaust volumetric flow rate was 1.6 m^3/s.

Figure 13 shows temperature contours on a vertical plane passing through the fire plume and Figure 14, contours on a vertical plane passing through the exhaust vent. The contours show that near the ceiling, the temperature is approximately

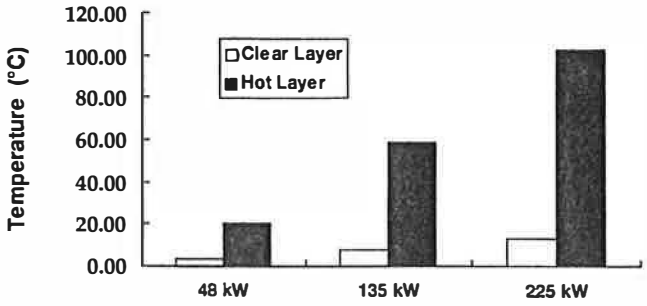

Figure 8 *Effect of heat release rate on layer temperatures. Graph of average temperature for three cases with exhaust vent on ceiling.*

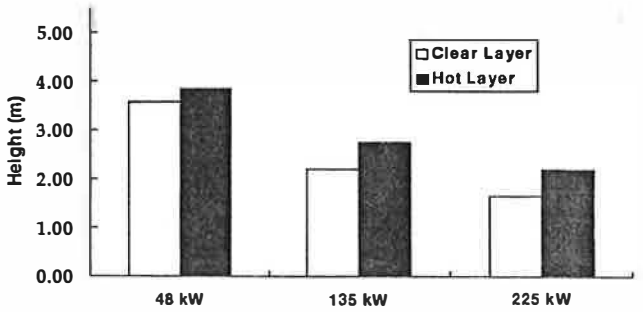

Figure 9 *Effect of heat release rate on layer heights. Clear and hot layer height for three cases with exhaust vent on ceiling.*

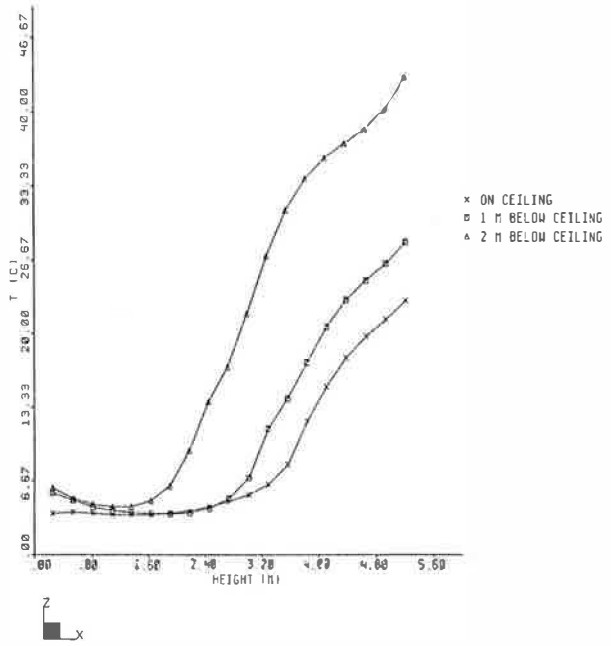

Figure 10 *Effect of vent location on temperature profiles.*

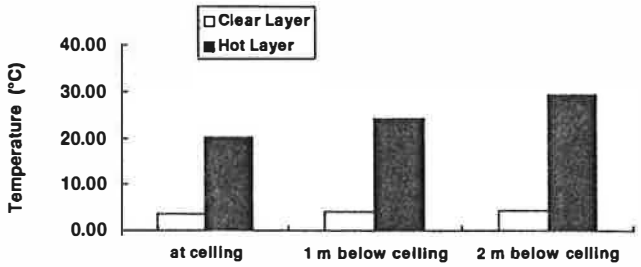

Figure 11 *Effect of vent location on layer temperatures. Average temperature of clear and hot layer for three cases with HRR = 55 kW.*

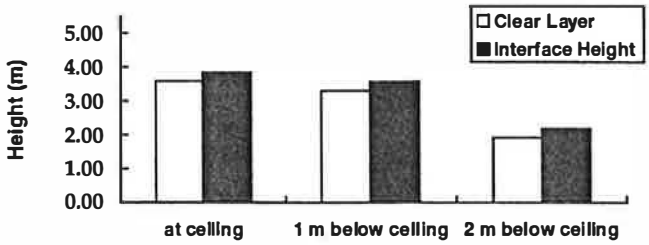

Figure 12 *Effect of vent location on layer heights. Clear and hot layer heights for three cases with HRR = 55 kW.*

TABLE 2
Runs Performed Modeling Fire Using a Volumetric Heat Source

Exhaust Location	Case	HRR (kW)	Clear Layer Height (m)	Hot Layer Height (m)	Clear Layer Temp. (°C)	Hot Layer Temp. (°C)
Vent at Ceiling	16	1	3.11	3.83	18.15	18.24
	17	5	4.30	4.54	18.17	19.63
	18	10	4.07	4.30	18.27	21.61
	19	25	3.59	3.83	18.49	26.81
	20	50	2.39	3.35	18.95	36.76
	21	225	0.72	1.44	24.02	119.78
Vent 1.0 m Below Ceiling	22	5	4.07	4.30	18.26	20.60
	23	10	3.83	4.07	18.31	22.30
	24	25	3.35	3.83	18.44	28.10

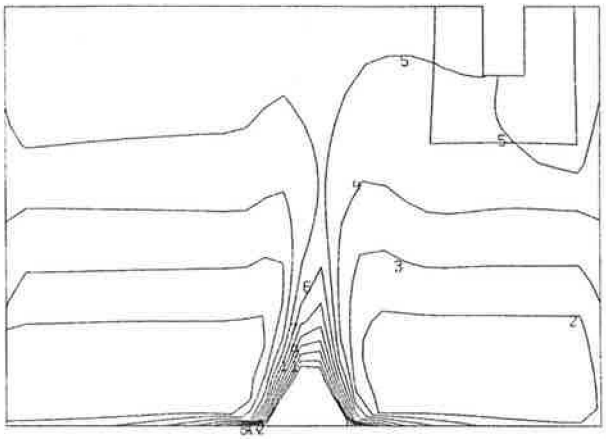

Figure 13 *Temperature contours for large scale through fire plume; contour 2 at 36.36°C and temperature difference between contours 26.36°C.*

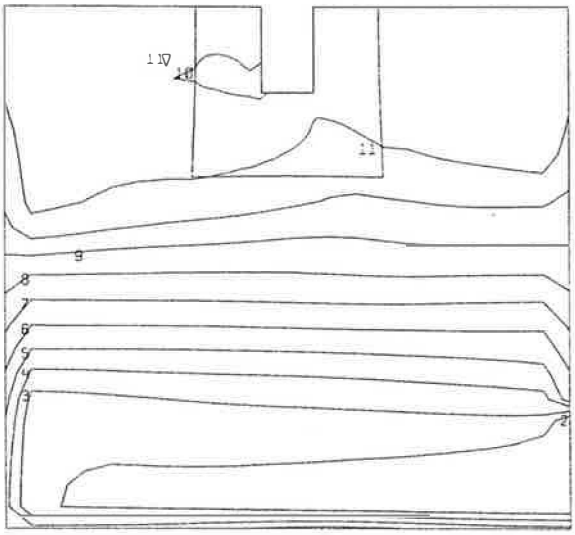

Figure 14 *Temperature contours for large scale through ceiling vent; contour 2 at 20.65°C and temperature difference between contours 10.65°C.*

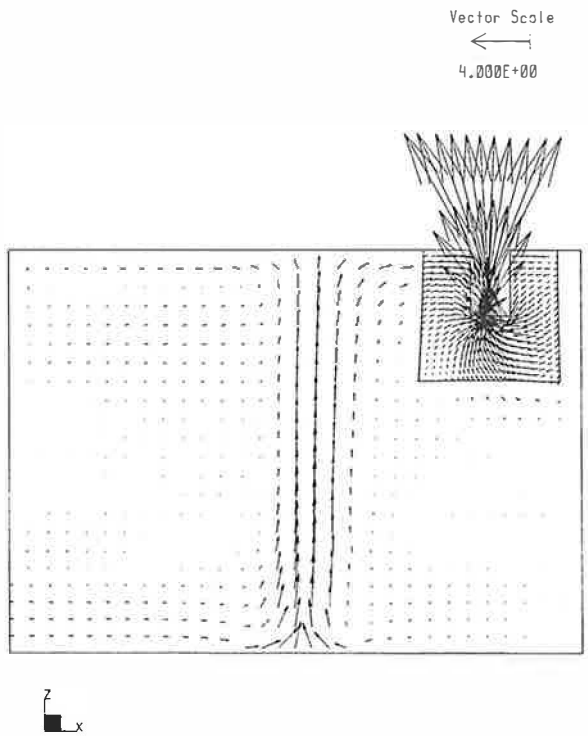

Figure 15 *Velocity vectors for large scale through fire plume (m/s).*

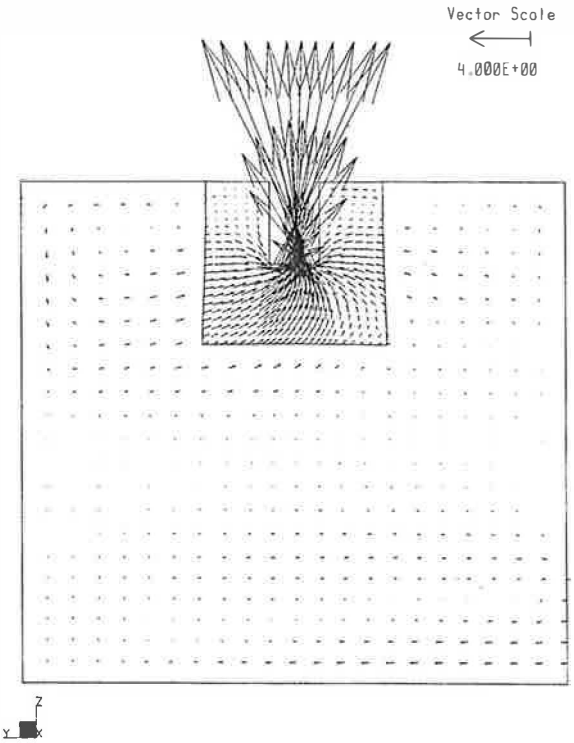

Figure 16 *Velocity vectors for large scale through ceiling vent (m/s).*

118°C and that the temperatures are uniform in each horizontal plane.

The velocity vectors for this simulation are shown in Figures 15 and 16. Figure 15 shows the velocity vectors on a vertical plane passing through the fire plume and Figure 16 shows the vectors on a plane passing though the exhaust vent. The vectors show that high velocities exist in the fire plume and at the exhaust vent. The exhaust system produces high velocities that influence the upper layer region, creating a strong recirculation zone. The lower part of the facility is quiescent with velocities less than 1 m/s.

Figure 17 compares predicted temperature profiles at the quarter point of the compartment with experimental data obtained at the same location and reasonable agreement is seen. However, the trend seen in the small-scale simulations is also seen in the large-scale simulations. While the experimental data show a clear distinction between the lower cold layer and the upper hot layer, with the upper layer having a nearly uniform temperature, the predicted results do not show a clear distinction. The predicted temperature increases with height and reaches a plateau near the ceiling. The experimental temperatures are higher near the interface and decrease with height from the interface. This temperature profile is possibly the result of the recirculation zone produced by the exhaust system.

Simulation of the Real-Scale Atrium

Both the small-scale and large-scale tests and simulations were models of real-size atriums. The scaling was done using Froude modeling. To investigate whether these scaling laws are applicable for compartments and fire intensities of this size, a run was performed using a real-scale atrium with dimensions of 24.2 m × 36.2 m × 44.0 m height. The fire size used for this simulation was 5 MW.

The results of this simulation are compared with the results from the reduced-scale model and are shown in Figure 18. The heights of the three simulations were normalized by dividing them by the total height of the atrium. The comparison of the temperature profiles indicates that the real-scale results compare very well with the small-scale numerical results. From this, it can be concluded that Froude modeling is applicable and can be used to do scale modeling of real-scale atria.

Modeling Parameters

To investigate the effect of fire area and height when the heat source approach was used in defining the fire, a number of runs were performed using the small-scale facility.

Figure 19 shows vertical temperature profiles at the room quarter point for four different fire heights: 1, 2, 4, and 8 control volumes. The heat release rate for these simulations was 225 kW. It is apparent from this graph that the fire height does not influence the results significantly. This is further illustrated in Figures 20 and 21, which show temperature and interface height for these cases. Similar results were obtained using a 50 kW heat release rate.

The fire area has a significant impact on the results, as shown in Figure 22. Although the maximum temperature in

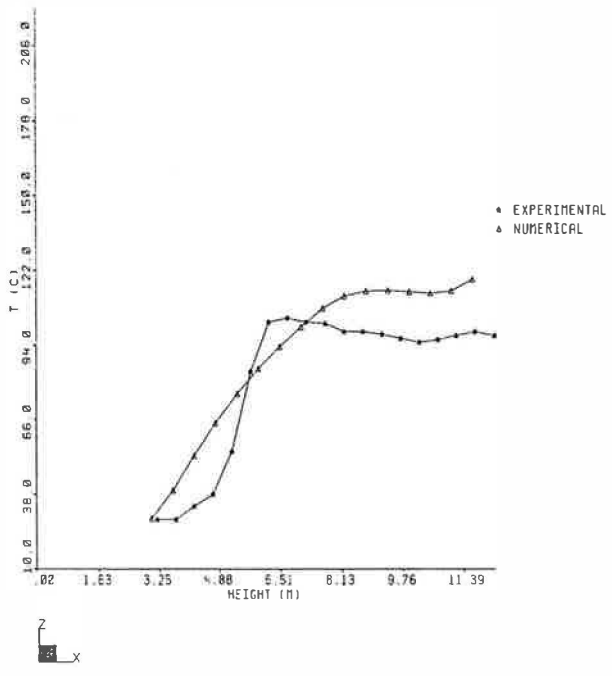

Figure 17 Comparison between predicted and experimental temperature profiles for large-scale model.

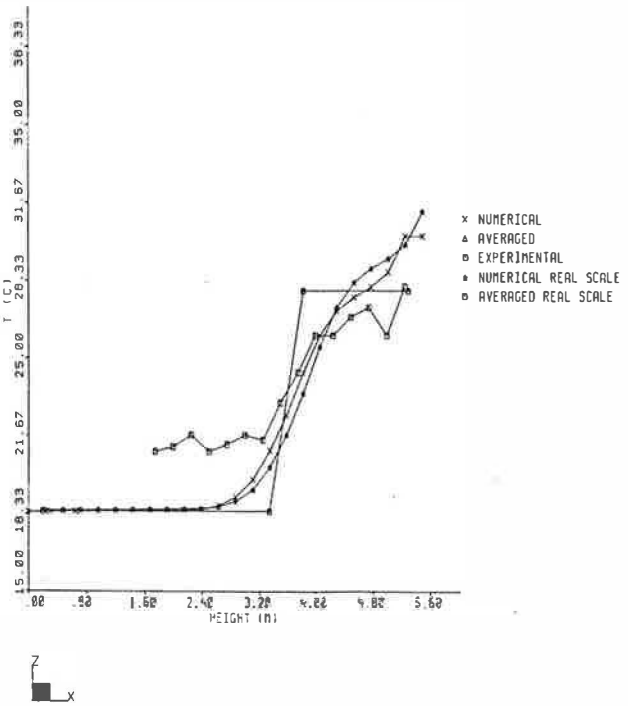

Figure 18 Comparison between real-size atrium and scale model.

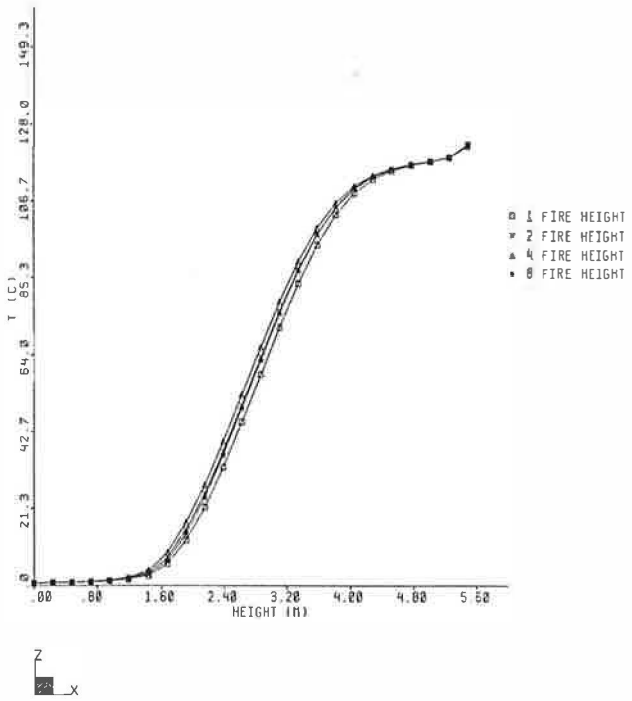

Figure 19 *Effect of fire height on temperature profiles.*

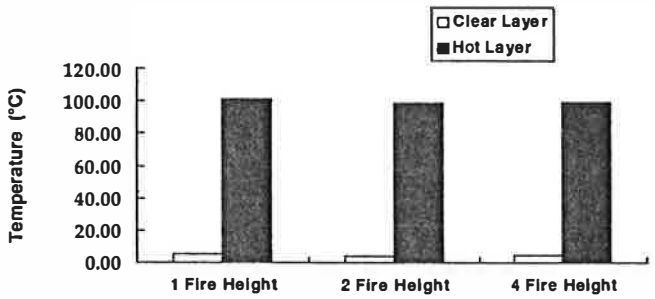

Figure 20 *Effect of fire height on layer temperatures. Average temperature for three cases with different heights of volumetric fire; HRR = 225 kW.*

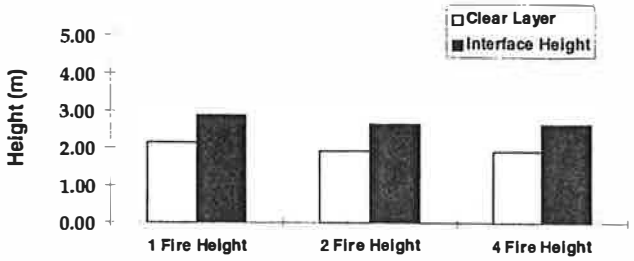

Figure 21 *Effect of fire height on layer height. Clear and hot layer heights for three cases with different heights of heat source; HRR = 225 kW.*

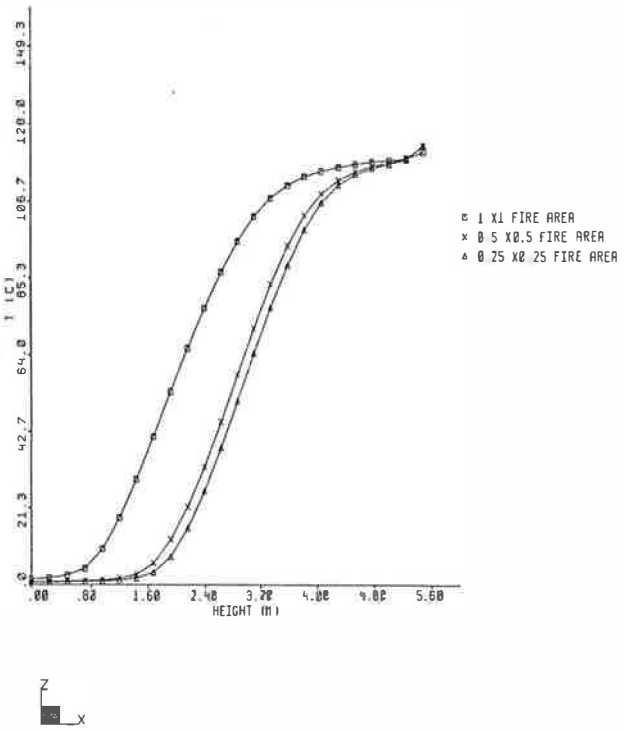

Figure 22 *Effect of fire area on temperature profiles.*

the room is the same for all runs, the profiles are quite different, resulting in different interface heights. Figure 23 shows the interface and clear heights in the room for the three cases. The interface height decreases as the fire area increases. This is expected because, with increased fire area, air entrainment into the fire plume increases, thus producing more smoke.

Figure 24 shows the average temperature in the hot and clear layers. The figure shows that the fire area does not affect the average layer temperature. Similar results were obtained when a heat release rate of 50 kW was used.

Simulations with Other CFD Models

One of the concerns with CFD models is whether their results are realistic. Because of the number of variables and parameters used in these models, it is often argued that any result can be produced by varying the input data. To determine whether this is true, two other CFD models were used to simulate one of the experimental tests. The runs with these two models were conducted at a university. The names of the models used are not shown.

Figure 25 compares the temperature profiles at the room quarter point determined by the two CFD models with the combustion model and with heat source and the experimental data. One of the models was able to predict uniform temperature within the hot layer. However, that temperature was much higher than the experimental temperatures. A second model predicted a profile in which the transition from the hot layer to the upper layer was very gradual. Temperature differences in this zone between the predicted results and the experimental data are quite high, with the predictions being 40% to 50% less than the experimental data. The other two predicted

results were closer to the experimental data. However, the temperature in the hot layer was not uniform, and the transition zone was not clearly defined as is in the experimental results.

These results support the concerns mentioned above and indicate the need for further work in identifying the parameters critical to atrium smoke management simulations. The results of this exercise are also consistent with results of an exercise performed by a CIB W14 subcommittee whose initial results indicate that different results are obtained even when the same model is used by different users.

Overall Comparisons with Experimental Data

Figure 26 shows a comparison between the experimental and numerical upper-layer temperatures. Overall, the agreement between the two is good, with the model slightly over-predicting the temperature. Figure 27 shows a comparison between the experimental and numerical CO_2 concentrations. As with the temperature results, this correlation shows that the model can predict CO_2 concentrations in the upper layer. Figure 28 shows a correlation of experimental and numerical interface heights. As shown, there is some scattering of the results; however, a similar scattering of the interface heights was observed in the experimental data.

Hot Layer and Duct Temperatures

Figure 29 shows a comparison between the calculated upper layer and exhaust temperatures. Under effective operating conditions, the exhaust system is expected to draw gases

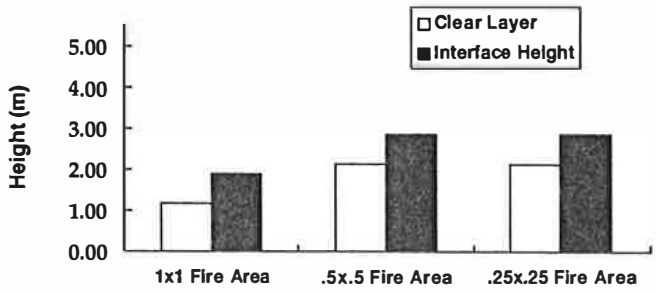

Figure 23 Effect of fire area on layer temperatures. Clear and hot layer heights for three cases with different fire areas; HRR = 225 kW.

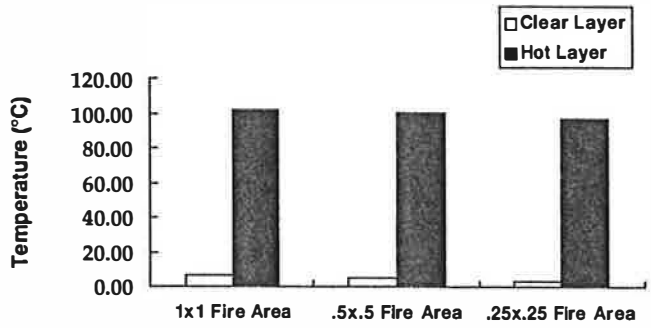

Figure 24 Effect of fire area on layer height. Average temperature for three cases with different fire areas; HRR - 225 kW.

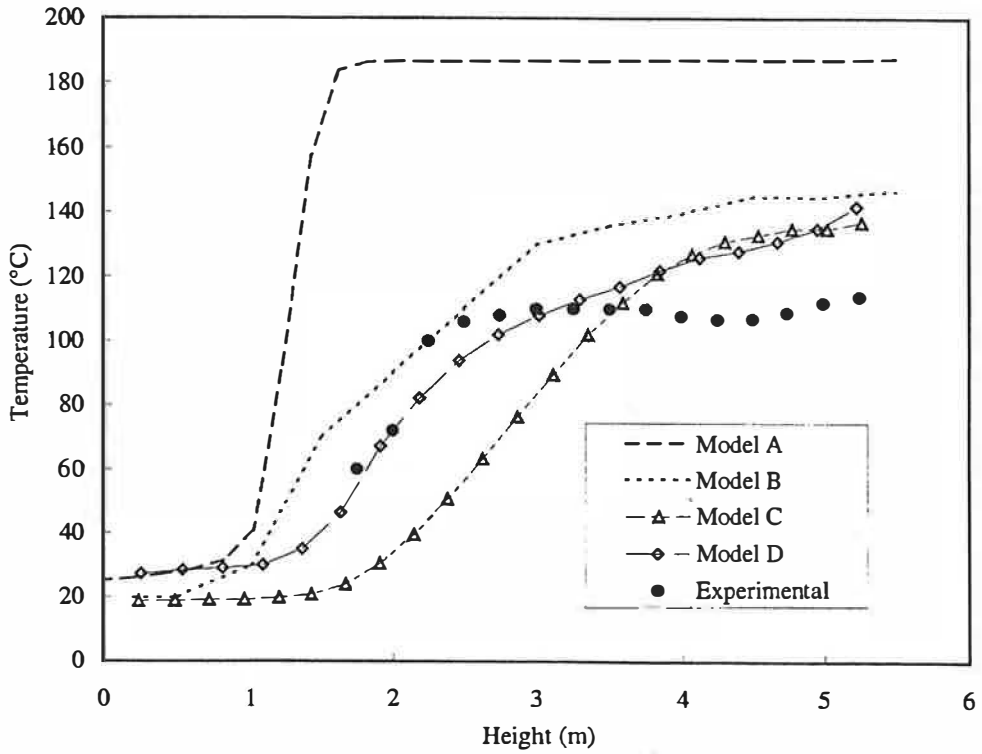

Figure 25 Comparisons of temperature profiles obtained from different CFD models.

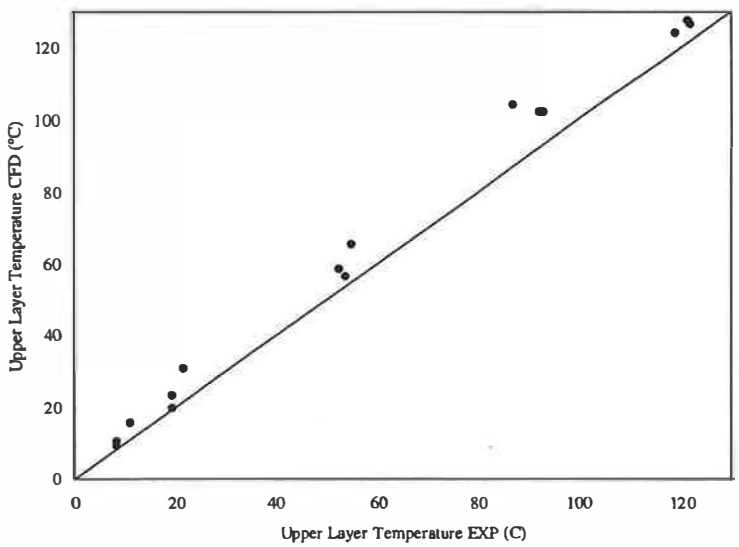

Figure 26 *Correlation of experimental and numerical temperature in upper layer.*

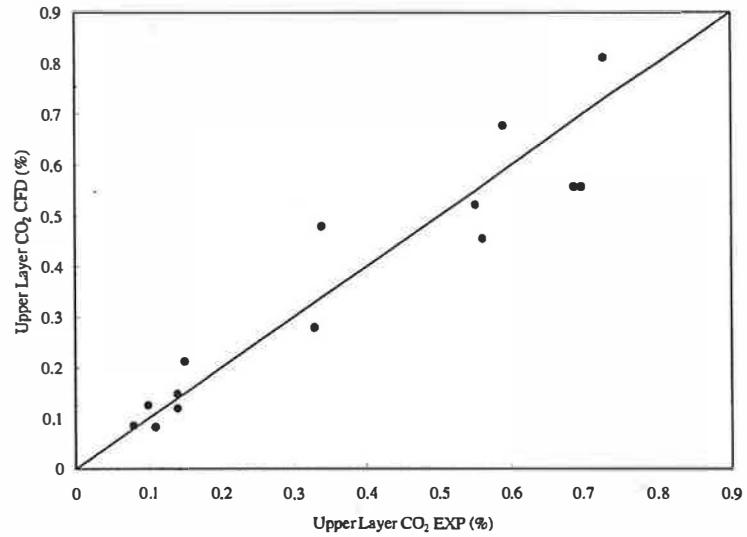

Figure 27 *Correlation of experimental and numerical CO_2 in upper layer.*

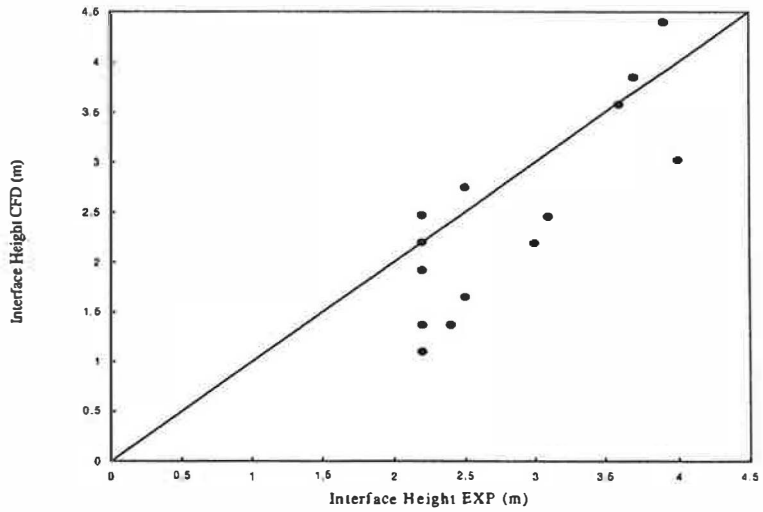

Figure 28 *Correlation of experimental and numerical interface heights.*

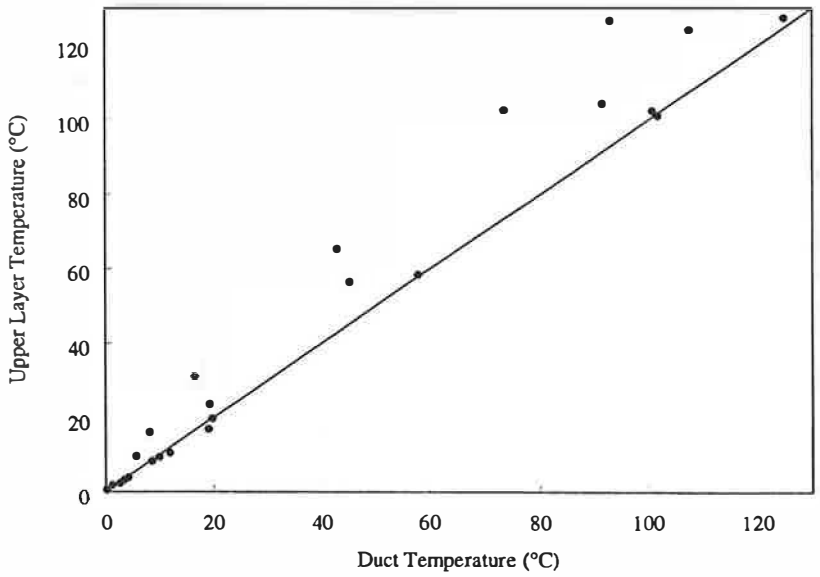

Figure 29 *Correlation of duct and upper-layer temperature for small-scale tests.*

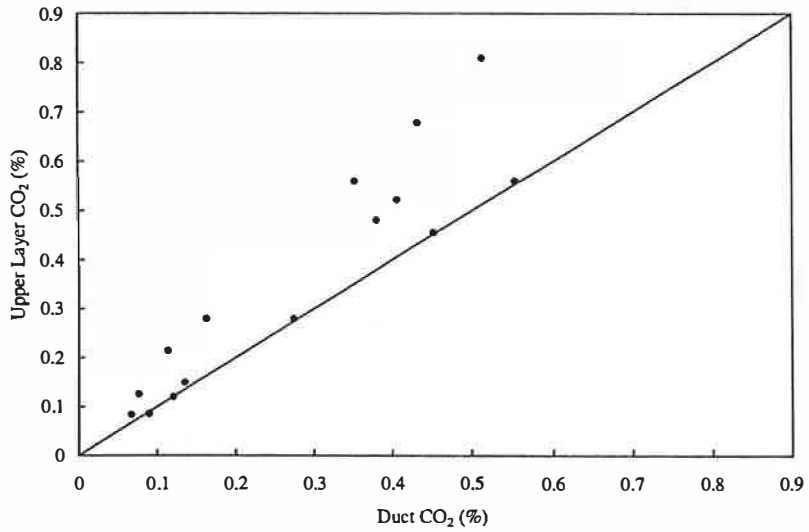

Figure 30 *Correlation of duct and upper layer CO_2 for small-scale tests.*

from the hot layer only, so the two temperatures are expected to be comparable. However, if the exhaust system draws in air from the cold lower layer, then the temperature in the duct will be lower than the temperature of the upper layer. As seen from Figure 29, the duct temperature for a number of cases is lower than the temperature of the upper layer, indicating that cold air is probably drawn into the exhaust system.

Similarly, Figure 30 shows a comparison between the calculated duct CO_2 concentrations and the CO_2 concentration in the upper layer. This plot confirms what is seen in Figure 29, that for some cases cold air is drawn into the exhaust system. The cases that resulted in cold air being drawn into the exhaust system were cases in which the flow rate of hot gases entering the hot layer was less that the fan flow rate. Although the efficiency of the exhaust system can be reduced in these cases, the system was still effective in extracting smoke from the space and maintaining an acceptable clear height. For the cases where there was a balance between the two airflow rates, the exhaust system was found to be not only effective but also efficient. That is, the air drawn into the exhaust system was predominantly from the upper hot layer.

Comparisons with Two-Zone, CFD Model, and Simple Correlations

Tables 3 and 4 compare experimental data with results from the CFD model, the simple correlations of ASMET (Klote 1994), and the two-zone model (Peacock et al. 1993). Comparisons are made for the interface height (Table 3) and for the hot layer temperature (Table 4). In general, the CFD

TABLE 3
Comparison of Interface Heights

HRR (kW)	Exhaust Rate (kg/s)	Experiments (m)	CFD (m)	ASMET (m)	CFAST (m)
22	1.19e-4	4.0	4.6	4.7	3.1
48	2.59e-4	3.5	3.8	3.9	2.7
135	7.28e-4	1.8	2.2	3.0	2.2
225	1.21e-3	2.3	1.5	2.4	2.0
280	1.51e-3	2.1	1.3	2.1	1.8

TABLE 4
Comparison of Hot Layer Temperatures

HRR (kW)	Exhaust Rate (kg/s)	Experiments (°C)	CFD (°C)	ASMET (°C)	CFAST (°C)
22	1.19e-4	26	26	25	25
48	2.59e-4	38	36	34	33
135	7.28e-4	63	68	72	61
225	1.21e-3	110	107	132	90
280	1.51e-3	132	130	186	107

results seem to overpredict the interface height for the lower heat release rates and underpredict it for the higher ones. The ASMET results compare very well with the experimental data, while the results from the two-zone model consistently underpredict the interface heights.

As shown in Table 4, the hot layer temperatures predicted by the CFD model compare well with the experimental data. ASMET predictions of the hot layer temperatures are good for the lower heat release rates, but they are higher than the experimental values for the higher heat release rates. Finally, the two-zone models consistently underpredicted the hot layer temperatures.

CONCLUSIONS

This paper presents numerical results obtained from a CFD model used to investigate the effectiveness of atrium smoke exhaust systems and compared the numerical predictions with experimental data obtained from physical model tests. In general, the comparisons indicated that the predicted hot layer temperatures and interface heights compare well with the experimental values. However, the temperature profile comparisons showed significant differences. The experimental data showed that the temperatures in the upper layer are quite uniform. The predicted temperatures, however, were not uniform. In addition, the results of the numerical simulation, performed using a real-scale atrium, showed that Froude modeling can be used to scale atrium systems.

Comparisons were also presented between results of the two-zone model and empirical correlations. Both the results of the empirical correlations and the two-zone model compared well with the experimental data.

REFERENCES

ASC. 1994. *TASCflow user documentation, Version 2.3.* Waterloo, Ontario: Advanced Scientific Computing, Ltd.

BOCA. 1996. *The BOCA national building code.* Country Club Hills, Ill.: Building Officials and Code Administrators International Inc.

Cooper, L.Y., M. Harkleroad, J. Quintiere, and W. Rinkinen. 1982. An experimental study of upper hot layer stratification in full-scale multiroom fire scenarios. *Journal of Heat Transfer*, 104: 741-749

Hadjisophocleous, G.V., G.D. Lougheed, C. McCartney, B.C. Taber, and S. Cao. 1998. *Design approach for atrium exhaust effectiveness, ASHRAE RP-899.* Ottawa, Ontario: National Research Council of Canada

Hansell, G.O., and H.P. Morgan. 1994. *Design approaches for smoke control in atrium buildings, BR-258.* Garston, UK: Building Research Establishment.

Heskestad, G. 1984. Engineering relations for fire plumes. *Fire Safety Journal*, 7: 25-32.

Hinckley, P.L. 1995. Smoke and heat venting. *SFPE Handbook of Fire Protection Engineering.* pp 3-160-3-173. Quincy, Mass.: National Fire Protection Association.

ICBO. 1994. *The uniform building code.* Whittier, Calif.: International Conference of Building Officials.

Klote, J.H. 1994. Method of predicting smoke movement in atria with application to smoke management. NISTIR 5516. Gaithersburg, Md.: National Institute of Standards and Technology.

Klote, J.H., and J.A. Milke. 1992. *Design of smoke management systems.* Atlanta: American Society of Heating, Refrigerating and Air-Conditioning Engineers, Inc.

Lougheed, G.D, and G.V. Hadjisophocleous. 1997. Investigation of atrium smoke exhaust effectiveness. *ASHRAE Transactions* 103: 1-15.

Lougheed, G.D, G.V. Hadjisophocleous, C. McCartney, and B.C. Taber. 1999. Large-scale physical model studies for an atrium smoke exhaust system. *ASHRAE Transactions* 105(1).

McCaffrey, B.J. 1983. Momentum implications for buoyant diffusion flames. *Combustion and Flame*, 52: 149-167.

Morgan, H.P., and J.P. Gardiner. 1990. *Design principles for smoke ventilation in enclosed shopping centres, BR186.* Garston, U.K.: Building Research Establishment.

NFPA. 1995. *NFPA 92B, Guide for smoke management systems in malls, atria, and large areas.* Quincy, Mass.: National Fire Protection Association.

Peacock, R.D., and V. Babrauskas. 1991. Analyses of large-scale fire test data. *Fire Safety Journal*, 17: 387-414.

Peacock, R.D., G.P. Forney, P. Reneke, R. Portier, and W.W. Jones. 1993. CFAST, The consolidated model of fire growth and smoke transport. *NIST Technical Note 1299.* Gaithersburg, Md.: National Institute of Standards and Technology.

Peters, N. 1984. Laminar diffusion flamelet models in non-premixed turbulent combustion. *Progress in Energy and Combustion Science*, 10(3): 319-339.

Peters, N. 1986. Laminar flamelet concepts in turbulent combustion. *21st Symposium (International) on Combustion/The Combustion Institute*, pp. 1231-1250.

Poole, G. 1997. CFD analysis of smoke movement in an atrium. ASC Report 30-1053-97.

Spratt, D., and A.J.M. Heselden. 1974. Efficient extraction of smoke from a thin layer under a ceiling. *Fire Research Note No. 1001.* UK Joint Fire Research Organization.